Scalable Computing: Practice and Experience, ISSN 1895-1767, http://www.scpe.org
© 2022 SCPE. Volume 23, Issues 4, pp. 211–223, DOI 10.12694/scpe.v23i4.2021

PREDICTION OF NAC RESPONSE IN BREAST CANCER PATIENTS USING NEURAL NETWORK

SUSMITHA UDDARAJU *, G. P. SARADHI VARMA† AND M. R. NARASINGARAO‡

Abstract. Breast cancer is now the most prominent female cancer in both developing and developed nations, and that it is the largest risk factor for mortality worldwide. Notwithstanding the well-documented declines in breast cancer mortality during the last twenty years, occurrence rates continue to rise, and do so more rapidly in nations where rates were previously low. This has highlighted the significance of survival concerns and illness duration treatment. Patient data after first chemotherapy is collected from the hospital and this data is then analysed using neural network. Proposed architecture gives result as the patient is responding to the chemotherapy or not. Moreover, it also gives the risk factor in surgery. Early prediction of such things gives broader idea about how treatment should go. Once the Breast cancer is detected and if chemotherapy is done, then it becomes very important to check whether patient is responding to the chemotherapy or not. So, the proposed system architecture is designed in such a way that it detects if the patient is responding to the chemotherapy or not. And if patient is not responding to the chemotherapy, then patient should go to the surgery. The proposed system is also compared with the existing algorithms machine learning and neural network techniques like support vector machine (SVM) and Decision Tree(DT) algorithms. The proposed neural network architecture gives 99.19% accuracy where SVM and DT gives 89.15% and 74.82%. Bosom disease is known to have asymptomatic stages, which is distinguished simply by mammography and around 10% of patients getting mammography recovers further assessments, and among them 8 to 10% require bosom biopsy. Alert the cautious consideration of the radiologist to peruse mammograms to perceive mammograms is generally 30 to 60 seconds for every picture. In any case, the weakness and explicitness of human radiologist's mammography was controlled by 77-87% and 89-97%, individually. As of late, twofold peruses are allowed with most screening programs, yet this will additionally disintegrate the time heap of human radiologists. As of late, the headway of man-made brainpower (AI) has made it conceivable to recognize programmed infection on clinical pictures in radiology, pathology, and even gastrointestinalities. For bosom malignant growth screening, all the more profound examinations have additionally been led, 86.1 to 9.0% responsiveness and 79.0 to 90.0% exceptional elements. By and by, there are a couple of distributions for built up disease location of mammography under Asian with higher bosom thickness contrasted with white individuals. Bosom thickness can influence the malignant growth pace of mammography pictures. Hence, the motivation behind this study was to create and approve a profound learning model that consequently recognizes threatening bosom sores in Asian advanced mammograms and to inspect the exhibition of the model by bosom thickness level. We have acquainted our own pretreatment technique with expand the exhibition of the model. Furthermore, we tried to lead a meta-examination to contrast and accessible investigations on AI-based bosom malignant growth recognition. Apparently, this is probably the greatest review done on Asians.

Key words: Neural network, chemotherapy, Residual Cancer Burden (RCB), Pathologic complete response (PCR)

AMS subject classifications. 68T05

1. Introduction.

Bosom malignant growth has turned into the most far and wide female disease in both creating and created countries, and it is the biggest reason for death among ladies nations from one side of the planet to the other [1]. Therapies for this sort of disease are agonizing, tedious, and may not be guaranteed to guarantee that malignant growth some way or another doesn't spread to different pieces of the body. As an outcome, different scholastics are attempting to more readily grasp the connections that exist in this confounded issue and to track down viable answers for work on the possibilities of treatment adequacy and, as an important result, the personal satisfaction of ladies who truly are going through it. [2]. The series of investigates on the attainability of therapies for bosom disease in ladies is increasing at similar rate as the quantity of instances of contamination around the world. As a reaction, clinical analysts are being completed in a joint effort with specialists in the factual or computational fields to mirror shrewd models equipped for rearranging and

*Research Scholar, Department of CSE, Koneru Lakshmaiah Education Foundation, Vaddeswaram, AP, India. (susmithauddaraju@yahoo.com).
†Professor, Department of CSE, Koneru Lakshmaiah Education Foundation, Vaddeswaram, AP, India.(gpsvarma@gmail.com).
‡Professor, Department of CSE, Gandhi Institute of Technology and Management, Visakhapatnam, India. (rmanda@gitam.edu).

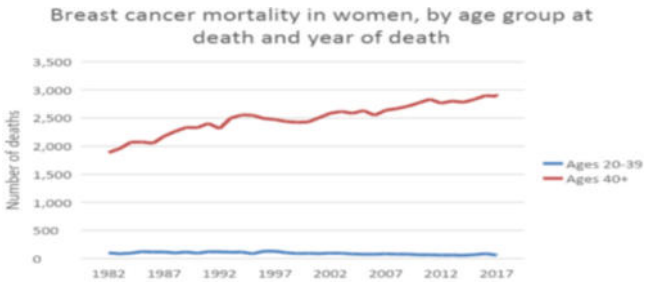

Fig. 1.1: Breast cancer incidence rates by age

demonstrating the viability of bosom disease medicines. In research, studies have been embraced to evaluate mental components of disease treatment and its relationship to treatment confidence, post-treatment impacts, connections, and effects on sleep deprivation. [3]. A few investigations take a gander at how people who have sought through treatment think [4]. One more ongoing line of examination investigates how comorbidities, age, and time since analysis impact therapy in the early discovery of disease [5] and, at long last, the effect of chemical substitution treatment on bosom disease cell development in menopause. The viability of bosom malignant growth medicines can be inspected from various perspectives, including social, monetary, and ladies' wellbeing. It is basic, be that as it may, to feature the significance of examination in view of information gathered from explicit patient gatherings. Teng et al. [6] learned at the bosom malignant growth instances of 5,279 ladies with invading pipe and lobular carcinoma. They were analyzed somewhere in the range of 2006 and 2010, and their data was assembled from the National Cancer Institute's SEER Cancer Registry. The first review intended to utilize Bayesian induction based prognostic displaying. In figure 1.1 we can see worldwide breast cancer incidence rates by age in women's. Here we can observe that the women above the age 40 are highly diagnosed with breast cancer [22].

Fluffy brain organizations (FNN) perform well when it connects with recovering attributes and relationships utilizing information bases in regards to clinical medicines. Canny half and half models have been used to expect emphaticness engine issues in youngsters [7] and to screen fetal wellbeing [8]. Classifier for the segmentation is stated by the Ajay Ladkat et al [9]. Different models were utilized to recognize mental imbalance in youngsters [10], grown-ups [11], and teenagers [12] utilizing electroencephalography (EEG).

At long last, it tackled difficulties in anticipating bosom malignant growth considering other assessment standards proposed by Silva Araujo et al. [13], for example, resistin, hyperglycemia, age, and BMI. Subsequently, utilizing Lymph Node Ratio Estimation investigation, such a methodology can work emphatically in the distinguishing proof of bosom malignant growth Survival Prognosis. Different AI approaches are tended to in paper by S. L. Bangare et al. [17], alongside numerical clarifications and instances of their utilization in genuine circumstances. S. L. Bangare et al. exhibited amazing review utilizing AI approaches in their distribution. K. Gulati et al. [18] and LMI Leo Joseph et al. [19] led research utilizing AI and profound learning draws near. Shachi Mall et al. [21] shown the utilization of Machine learning for sickness discovery and so on. The creators have introduced most ideal component extraction methods for shape portrayal and utilized the Neural Networks, for example, Capsule Network, KNN for the grouping.

The primary commitment of this paper is to configuration new methodology for the characterization of impacts after the hemotherapy. The paper comprises of the proposed framework engineering alongside the measurements. The outcomes have been checked and confirmed from the master specialists. Likewise, the proposed framework's outcomes have been contrasted and existing framework and there similar diagram is additionally plotted in outcome meeting. At last, decisions about the exercises acted in the paper is introduced in last meeting.

Patients who went through cutting edge bosom mammography and endocrine treatment were signed up for this survey. Just subjects beyond 18 years old who were not associated with the technique were enlisted. Distant clinical records, no necessary affirmation of dubious bosom injury, missing mammograms, or the idea of

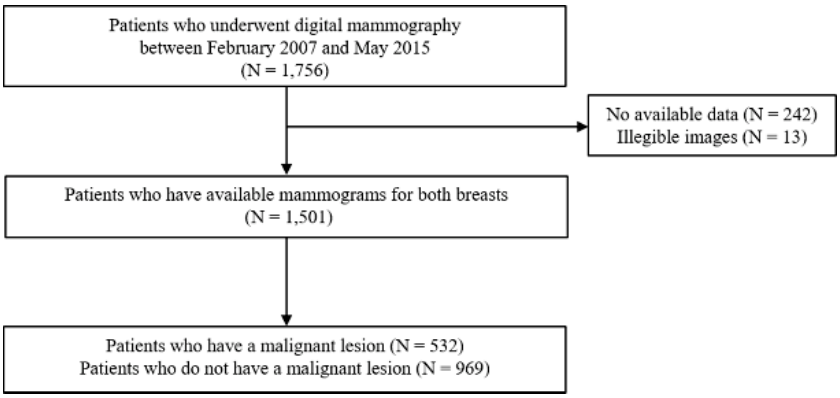

Fig. 1.2: Flow diagram

mammograms can't be translated true to form because of unsettling, defocus, or irritating spots. Low subjects were prohibited [1]. This study was supported by the Institutional Review Board (No. 201903004) and consented to the rules of the Helsinki Declaration. Board for Institutional Review has removed the prerequisite for designed informed assent on the grounds that the survey represents an immaterial gamble to the issue. Skulls and normal along the side slanted mammograms of each bosom were gotten from taking an interest subjects utilizing a photo placement and relating outline and # 40. Hallym University Sacred Heart Hospital focusing on PACS and # 41; 2560x3328 pixels. The computerized mammography convention is agreeable with the European Federation of Medical Physics Organizations. All pictures were taken utilizing a Lorad Selenia PC mammography apparatus (Hologic Incorporated, Bedford, USA). The display of the unit was guaranteed inside the predefined flexibility's brought out for quality control all through the assessment period [2]. Individual information, clarifications, or showed information that portrays the possibility of the laterality or mammography view has been taken out from the picture, Every mammography was then re-examined two radiologists, also checked for the presence of undermining wounds. Clinical records of possibly threatening bosom sores, past mammography estimations, and neurotic reports were reflectively explored and followed up for no less than 5 years after mammography assessment. Threatening sores must be affirmed by careful histopathology. The support flowchart is introduced in Figure 1.2.

2. Related works.

2.1. Data Preprocessing. All pictures were resized to 1000x1300 pixels before investigation. The pictures were then preprocessed with the CLAHE calculation (contrast-restricted versatile histogram evening out) to limit contrast contrasts between the pictures [3]. CLAHE is an adjusted form of versatile histogram balance. This is a picture handling calculation that changes the brilliance of every pixel in a picture and applies histogram adjustment locally to contiguous pixel regions to work on the nearby differentiation of the picture [4]. The CLAHE calculation tackles the clamor over amplification issue of versatile histogram evening out by restricting the incline of the combined thickness work while ascertaining histogram adjustment [5]. In this review, CLAHE was carried out utilizing the Python programming language OpenCV library rendition 4.1.2.30. We flipped every one of the mammograms of the left bosom upward and gave the picture an organization like that of the right bosom to make a bound together profound learning model for the right and left bosoms. Then, for each bosom, the crania-caudal and average sidelong slanted pictures were trimmed to eliminate just 10% of the vacant space and associated evenly. At last, the size of the connected pictures has been changed to 900x650 pixels [6]. 1.2. Record structure All combined pictures were ordered into two classes, harmful and harmless, in view of the presence or nonattendance of threatening sores in the pictures. The whole dataset was parted into preparing and test datasets, and 10% of the pictures in every classification were haphazardly relegated to the test dataset. The remainder of the preparation datasets was then additionally partitioned into the right preparation and tuning datasets in an 8: 1 proportion utilizing arbitrary tasks by classification

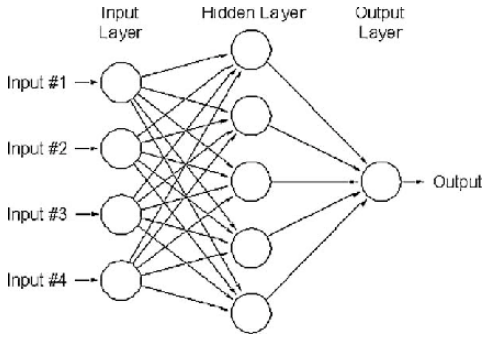

Fig. 2.1: Artificial Neural Network

[7]. The preparation, tuning, and test datasets were fundamentally unrelated and absolutely thorough. Since the dangerous growth bunch was around one-fifth the size of the non-harmful cancer bunch, the threatening growth bunch was extended in the preparation dataset to ease the class unevenness. Pictures of the threatening cancer bunch in the preparation dataset were amplified up to 5x, creating 10% and 20% amplified pictures of the dataset and 10% and 20% decreased pictures.

2.2. Training Convolutional Neural Networks (CNNs). Two CNN structures, DenseNet169 and EfficientNetB5, were utilized to foster profound learning models. Basically, DenseNet169 is a CNN structure highlighting high thickness impedes that are connected with the information include guides of each past sub block and utilized as the info highlight guide of a specific sub block [8]. This tight association tackles the disappearing angle issue and diminishes the quantity of boundaries [9]. EfficientNetB5 was planned utilizing MBconv blocks that all the while control the equilibrium of organization width, profundity, and goal through support learning [10]. This organization beats the picture arrangement organization of past ImageNet datasets with less boundaries and induction time [11]. Both of these CNN models prepared on the ImageNet dataset and optimized on the prepared dataset for this review. Using the Adam Optimizer, we used 0.9 for Beta 1 and 0.999 for Beta 2 to limit double cross entropy. The underlying learning rate was positive, and the learning rate decreased by 10 to 10 years until it reached 107. The group size was configured at 4, and the way racy factor was fine. Early stopping was applied after 30 years, with a 20-year tolerance. The dropout was not used for DenseNet169, but was used for EfficientNetB5 with a 0.4 dropout rate. The Pytorch structure was used in a handling unit designed by NVIDIA GeForce Titan RTX.

2.3. Gradient-Weighted Class Activation Mapping (Grad-CAM). Two CNN structures, DenseNet-169 and EfficientNetB5, were utilized to foster profound learning models. Basically, DenseNet169 is a CNN structure highlighting high thickness impedes that are linked with the info include guides of each past subblock and utilized as the information include guide of a specific subblock [12]. This tight association tackles the evaporating slope issue and diminish the quantity of boundaries [13]. EfficientNetB5 was arranged using MBconv blocks that meanwhile control the harmony of association width, significance, and objective through help learning [14]. This association beats the image game plan association of past ImageNet datasets with less limits and acceptance time [15]. Both of these CNN models pre-arranged on the ImageNet dataset and changed on the planning dataset for this audit. The Adam Optimizer was used to restrict equal with beta1 of 0.9 and beta2 of 0.999, compute cross entropy. The basic learning rate was OK, and the learning rate decreased by 10% every 10 ages until it showed up at 10-7. The bundle size was set to 4 and the weight decay factor was certifiable. Early stopping was used after 30 ages with diligence of 20. The dropout was not used for DenseNet169, but was used for EfficientNetB5 with a dropout speed of 0.4. The NVIDIA GeForce Titan RTX plans-handling unit utilises the Pytorch framework. A back spread mind network tends to a neuron and adjoining layers that are related by loads.

Equations (2.1) and (2.2), which describe how hidden nodes are activated, can be used to explain the

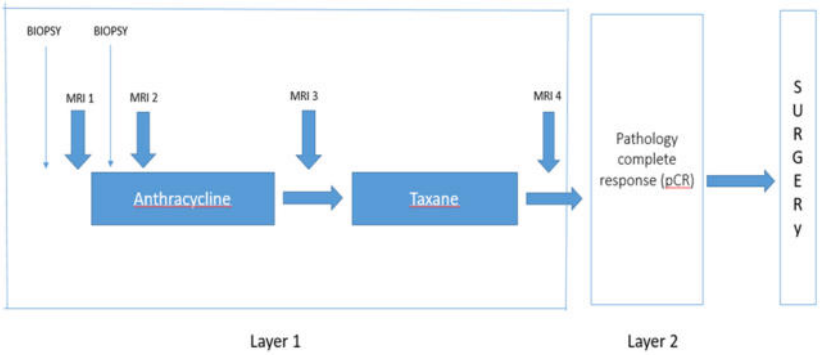

Fig. 3.1: Collection of Data

calculation.

$$I_j = \sum_i w_{ji} y_i + a_j \tag{2.1}$$

where, $f_j = activationfunction$

$$T_j = f_j < I_j \tag{2.2}$$

w_{ji} =weight attached to the nodes in input layer I and hidden layer j's connecting link
a_j =the predisposition related at every association connect between the information layer and secret layer.
y_I =contribution at hubs in input layer.
I_j =sum of the weight inputs multiplied by predisposition
T_j =result of initiation work at stowed away layer.
The guideline of result layer can be derived utilizing Eqn. (2.3) and Eqn. (2.4).

$$I_n = \sum_j w_{nj} y_j + b_n \tag{2.3}$$

$$T_n = f(I_n) \tag{2.4}$$

w_{nj} =weight related at the association interface between hubs in secret layer j and hubs in yield layer n.
b_n =the inclination related at every association interface between the secret layer and result layer.
y_j =yield at hubs in secret layer
I_n =summation of weighted yields at the result layer.
T_n =last result at the result layer.

3. Methodology. Patient data after first chemotherapy is collected from American Oncology Institute (AOI) Manglagiri, Guntur. American Oncology Institute (AOI), the best hospital for cancer in Vijayawada operates a full-fledged facility at NRI Hospital, Manglagiri. The data is collected in the form of an excel sheet. The dataset consists of 884 instances with 11 input features. The data is collected before, in-between and after Neo adjuvant chemotherapy(NAC) of the patient as shown in figure 3.1. The initial course of treatment for locally progressed breast cancer is neo adjuvant chemotherapy (NAC) (BC). Its major goal is to obtain a pathological full response in addition to making breast conserving surgery practicable (pCR) Input parameters of the dataset and its description are as stated in table 3.1.

Dataset contains patient socioeconomics and pre-treatment boundaries. Complete dataset is partitioned into the race of the patient, Estrogen Receptor Status (ERS), Progesterone Receptor Status (PRS), Hormone Receptor Status, Her2 classification Status, reciprocal bosom disease status, and record cancer laterality. Other

Table 3.1: Input parameters in database and their values

Input Parameters in database	Values of parameters
Race of the patient	Caucasian, African American, Asian, Native Hawaiian/Pacific Islander, American Indian/ Alaskan Native
Estrogen Receptor Status (ERS)	Positive or Negative
Progesterone Receptor Status (PRS)	Positive or Negative
Hormone Receptor Status	Negative if both ERS and PRS are Positive Positive if both ERS and PRS are Negative
Her2 category Status	Positive or Negative
Bilateral breast cancer status	Yes or No
Index tumour laterality	Left or Right

Table 3.2: Output parameters in database and their values

Output parameters in database	Values of parameters
pathological complete response (pCR)	Yes, No, or No surgery
Residual Cancer Burden (RCB) class	Class 0 to 3, No surgery

than this four more MRI features are used as input in this research. Totally 11 features are used as input features in this work. Race of the patient incorporates Caucasian, African American, Asian, Native Hawaiian/Pacific Islander, American Indian/Alaskan Native. Trama centers, PRS and Her2 status are either certain or negative. Chemical receptor status is negative in the event that the two ERS and PRS are negative, positive assuming ERS or PRS is positive. Patients either have reciprocal bosom disease before neoadjuvant treatment or not. File cancer laterality is left or right.

We cannot feed collected database directly to the neural without pre-processing. Some fields in the collected dataset are of the string type. So, by using linear encoding method the string is converted into the logical numbers. Proposed framework accepts these highlights as information. Then this information is taken care of in lined up with the thick layer with 16 and 64 neurons into it, etc as show in figure 3.2. By utilizing thick layer, the dimensionality of the vectors gets changed. Each neuron in the past layer is associated with each neuron in the following layer. Here for every layer except last layer activation function used is Relu. And in last layer activation function is softmax. The neural network is consisting of two parallel running convolution neural networks. It is the novelty of the proposed neural network that two neural network accepts the data simultaneously and gives one result.

Proposed system takes input features as input. Then the input is fed parallel to dense layer with 16 neurons and 64 neurons into it. 16 and 64 neurons are fed parallel to 64 and 16 neurons. 64 and 16 neurons are fed parallel to 128 and 32 neurons and so on as shown in figure 3.2. In the last layer the dimension changes from 2 to 1, which means the data is combined and only one result is taken out from the system. The outcome result is about chemotherapy response along with the criticality due to cancer tissue. By using the dense layer the dimensionality of vectors get changed. Every neuron in previous layer is connected to every neuron in the next layer. The activation function we used for this network is RELU except for the output layer. The activation function we used for output layer is SOFTMAX.

In the last layer the dimension changes from 2 to 1, which mean the data is combined and only one result is taken out from the system. The outcome result is about chemotherapy along with the criticality due to cancer tissues.

It gives an idea about how a patient responds to the Chemotherapy. If the patient does not respond to the chemotherapy, then it suggests the need for surgery. Residual Cancer Burden (RCB) class suggests the criticality of the patient after first Chemotherapy.

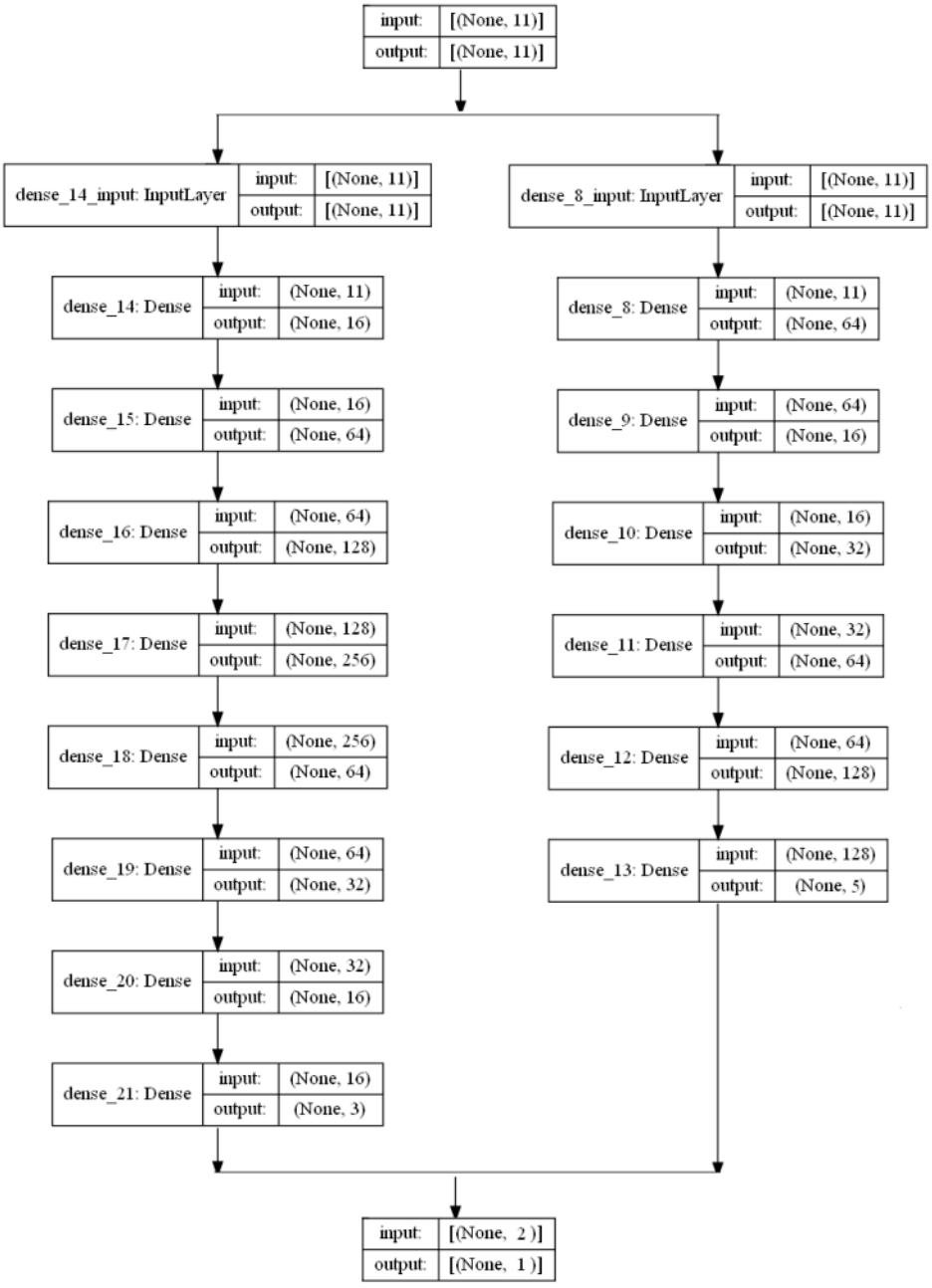

Fig. 3.2: Proposed system architecture

The Naive Bayes Classifier (NBC) is a very valuable Bayesian learning strategy. This classifier uses Bayes' hypothesis to accept freedom between indicators. Basically, NBC accepts that the existence of a property in one class is freed from the existence of another class. Bayesian hypothesis finds accidental probabilities. Numerically, this is in condition (1). (19). The factors of conditions (19), (20), and (21) are expressed as follows. I.) $P(Y|X)$ is the inverse likelihood of class Y given the indicator (X). II.) $P(Y)$ is the prior probability of the class. III.)

Table 3.3: Mammogram data composition

	Whole Dataset		Training Set		Test Set	
	Breast n	Patient n	Breast n	Patient n	Breast n	Patient n
Overall	3002	1501	2701	1484	301	284
Non-Malignant	2465	1496	2218	1427	247	235
Malignant	537	532	483	478	54	54
A	152	76	132	74	20	18
Breast B	594	297	532	292	62	57
density C	1560	780	1405	774	155	149
D	696	348	632	344	64	60

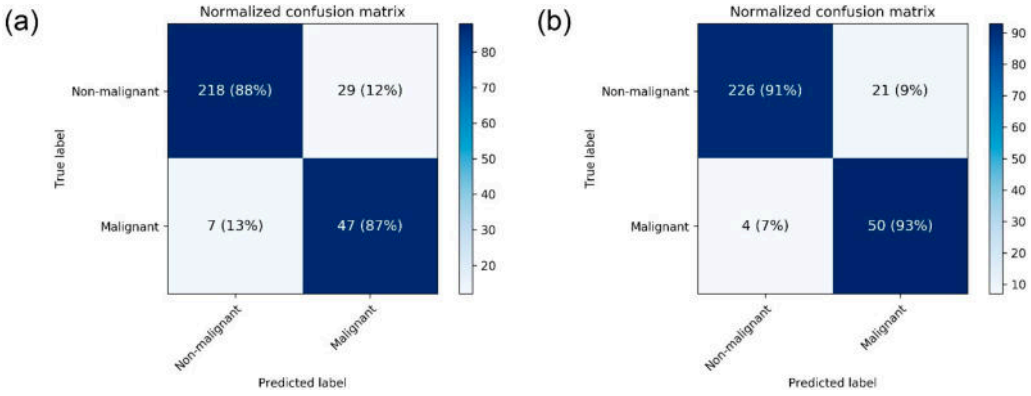

Fig. 3.3: Breast cancer detection heat map of confusion matrix

$P(X|Y)$ is the probability of the indicator, also known as the probability. IV.) $P(X)$ is the past probability of the indicator.

3.1. Clinical Subject Demographics. Finally, 3002 in total combination 1501 patients' mammograms were examined. recalled for review. The normal age of the members was 48.9 ± 11.1 years. The entire dataset contained 537 malicious images and 2465 non-malicious images [15]. The dangerous cancer group was more experienced than the non-dangerous growth (52.7 11.2 vs. 48.1 10.9 years; p 0.001) group. A number of many images of big breasts of thickness a C or a D (2256, 75.1 percent). Table 3.3 shows the information structure of the prepared and test datasets. The test dataset contained 54 images named Malicious Images and 301 images, including 247 non-vengeful images. The normal time for members to take mammograms on the 49.9 10.9 years made up the test dataset.

3.2. Detection of Breast Cancer by CNN Models' Performance. Table 3.3 shows the measurements for a typical CNN design exhibition. The recommended AUC for the most malignant breast growth location on the mammogram was changed to 0.952 ± zero half for the DenseNet 169 method and 0.954 ± 0.020 for the EfficientNet B5 method. The proposed accuracy was changed to 88.1 ± 0.2% for the DenseNet 169 method and 87.9 ± 4.7 for the EfficientNet B5 method. For the DenseNet169 model, the recommended responsiveness and specificity scores were 87.0 ± 0.0 and 88.4 ± 0.2, respectively. Figure 3.2 shows a standardized confusion framework for CNN structures that separates harmful images from harmless images.

4. Results and experimentation.

4.1. Grad-CAM. The results are tested on the image dataset also to verify the results collected in the form of excel sheet. The result of the classification for the image as input is shown in figure 3.3. Figure 4.1 shows an illustration of a GradCAM picture. The CNN model effectively distinguished harmful injuries. In

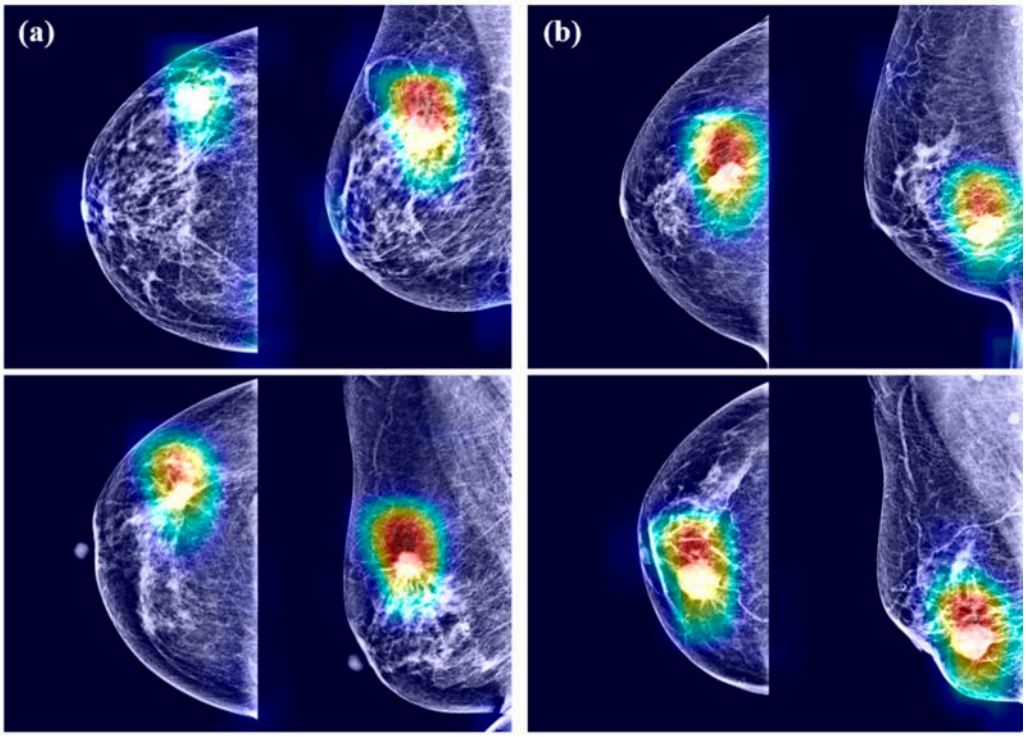

Fig. 4.1: Gradient-weighed class for mammograms by DenseNet-169 and (b) EfficientNet-B5

the combined mammogram, harmful sores were generally appropriately recognized in both caudal and average sidelong slanted sees. The CNN model zeroed in on the point of interaction between bosom disease and the encompassing parenchyma [16, 17, 18, 19]. Radiodensity regions offered more to disease forecast than radiation porous regions. Specifically, CNN models would in general recognize irregularities as mass and calcification instead of compositional mutilations and imbalances. Nonetheless, the radiation murky construction of the typical design was not thought of as being available in many images is logica GradCAM [20, 18, 19].

Look at the consequences of different grouping models and analyze them. It ought to be noticed that the outcomes showed in Table 4.1 have a mix of SVMLDA, NLDA, NNRFE, NNPCA, NLDA and NNRDA and NN alone, with the best exhibition of 99.07% in regards to explicitness. In any case, the blend of SVMLDA and the mix of NNLDA (98.41%), exactness (98.41%), update (98.41%), accuracy (98.41%), callback (98,41%), callback (98.41%) I got the best presentation as far as And precision (98.82%). The most unfortunate fitting ML model for responsiveness and review was a mix of Nb-CFS, and precision, particularity, exactness, Nb and Nb were scant of RFE pretreatment information. Likewise, dimensionalization influences the exhibition of the ML calculation. Reproduction results show that the CFS and RFE techniques work on the precision and particularity of the outspread piece SVM, and the LDA works on the two its exactness and awareness (discovery of threatening cases). For ANN, CFS increments awareness, and RFE, PCA, and LDA increment responsiveness and arrangement precision. NB exactness is CFS and LDA have improved, and awareness is upgraded by LDA. AI grouping calculations are additionally analyzed utilizing their particular ROC plots and the region underneath the kappa esteem. SVMLDA, NNLDA, and NBLDA had the best locales under the ROC bend. The worth is 0.9994 and its superior execution is shown. Furthermore, the best kappa worth of 0.9748 was gotten from SVMLDA and NLDA. Aspect decrease is vital in the arrangement cycle. Highlight extraction assumes a significant part in arrangement models. The primary motivation behind performing highlight extraction ought to work on prescient execution and guarantee quicker expectation. In this manner, the advantages of component extraction can't be overstated. Highlight extraction makes it simpler to envision

Table 4.1: Summary of machine learning models' results

Machine Learning Models	Accuracy	Area under ROC Curve	Precision	Recall	Sensitivity	Specificity	Kappa
SVM	0.9647	0.9964	0.9385	0.9682	0.9682	0.9626	0.9248
SVM-CFS	0.9647	0.9954	0.9524	0.9524	0.9524	0.972	0.9243
SVM-RFE	0.9637	0.9966	0.9534	0.9534	0.9534	0.962	0.9253
SVM-LDA	0.9872	0.9984	0.9871	0.9871	0.9871	0.9917	0.9448
NN	0.9746	0.9975	0.9733	0.9465	0.9465	0.9807	0.9463
NN-CFS	0.9606	0.9873	0.9431	0.9783	0.9783	0.9619	0.9472
NN-RFE	0.9724	0.9979	0.9739	0.9673	0.9673	0.9927	0.972
NN_PCA	0.9755	0.9947	0.967	0.9724	0.9554	0.9977	0.9592
NN-LDA	0.9782	0.9894	0.9741	0.9741	0.9741	0.9807	0.9748
NB	0.9218	0.976	0.885	0.8789	0.8789	0.9452	0.8015
NB-CFS	0.9276	0.9599	0.9052	0.8471	0.8471	0.9433	0.8711
NB-RFE	0.9118	0.986	0.875	0.8889	0.8889	0.9352	0.8115
NB-LDA	0.9724	0.9894	0.9739	0.9783	0.9583	0.9807	0.952

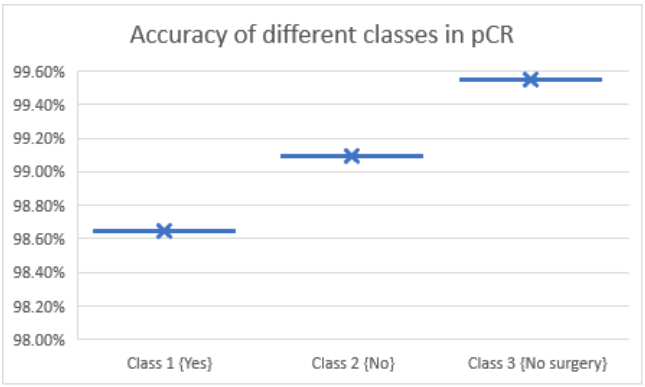

Fig. 4.2: Calculated accuracy of classes in pCR using proposed architecture

and get your information. Furthermore, highlight extraction lessens memory necessities and preparing time. Results are tested on different machine learning and neural network algorithms. From table 4.1 it is clear that the performance parameters of the machine learning algorithms are much lesser than that of the neural network algorithms. This is the reason behind selecting the neural network approach over machine learning.

Complete database is tested by using proposed architecture. It gives the around 99% accuracy for the prediction of pCR. The integrated 3 classes accuracy is visualized in figure 4.2. Accuracy for PCR classes of class 1, class 2 and class 3 are 98.62%, 99.10% and 99.55% respectively. As compared to other classes class 3 is having 99.5% accuracy which the highest. As the average accuracy of all the classes comes out to be 99%, it is highly reliable system.

Similarly, the same data is tested for RCB, and the accuracy for different classes is as them in fig 4.3. Accuracy for RCB classes of Class0, Class 1, Class 2, Class 3 and Class 4 are 99.55%, 100%, 98.20%, 99.10% and 99.55% respectively. It is shows that the class 1 is having the maximum accuracy while class 2 is having minimum accuracy. Except class 2, all the classes are having accuracy more than 99%.

The overall pCR and RCB classification accuracy come out to be 99.095022% and 99.276018% respectively. Precision value of pCR classification is higher than that of the RCB classification. In case of Recall and F1

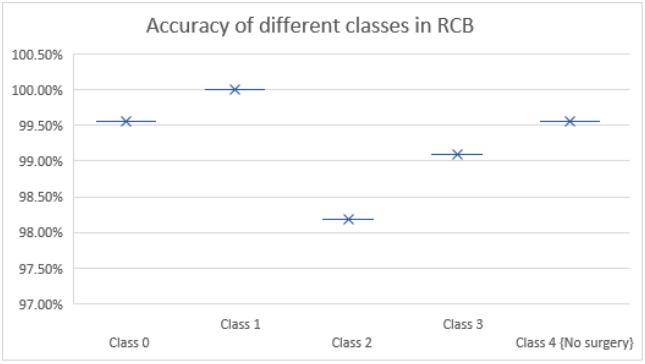

Fig. 4.3: Calculated accuracy of classes in RCB using proposed architecture

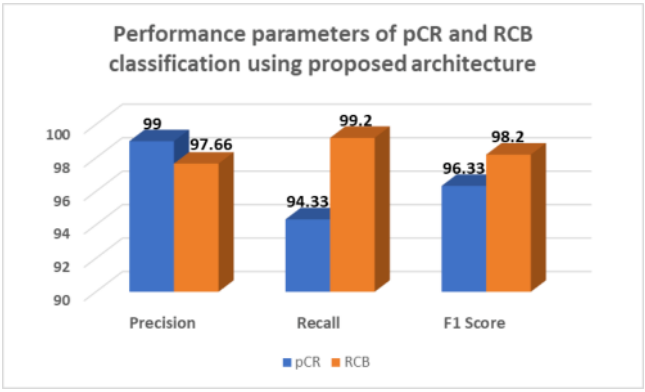

Fig. 4.4: Performance parameters of proposed architecture for classification of pCR and RCB

Table 4.2: Class wise performance parameters of pCR classification

Class	Precision	Recall	F1-Score
Class 1 {Yes}	99%	99%	99%
Class 2 {No}	98%	98%	98%
Class 3 {No Surgery}	100%	86%	92%

score value of RCB classification is higher than that of the pCR classification.

Table 4.2 and table 4.3 gives class wise performance parameters for pCR and RCB classification utilising the suggested architecture.

Precision, recall and F1 score of the class 1 is 100% it means changes of misclassification of class 1 is zero. Precision of class 1 and class 2 is maximum which is 100%. Except class 2 all the classes is having recall value is equal to 100%. The minimum value of F1 score is 97% for class 3 and class 4.

Same database is trained and tested using SVM and decision tree algorithm. Proposed system gives much higher accuracy than the SVM and decision tree algorithm.

Same database is trained and tested using different existing algorithms like naive bayesain, random forest, KNN, SVM and decision tree. But, in figure 4.5 presented comparsion with svm and DT because among all these two gave better performance. Proposed system gives much higher accuracy than the other existing algorithms.

Table 4.3: Class wise performance parameters of RCB classification

Class	Precision	Recall	F1-Score
Class 0	98%	100%	99%
Class 1	100%	100%	100%
Class 2	100%	96%	98%
Class 3	95%	100%	97%
Class 4 {No Surgery}	95%	100%	97%

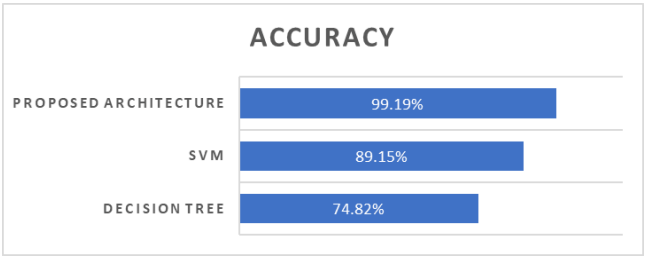

Fig. 4.5: Comparison of existing and proposed architectures

Table 4.4: The duration required to obtain data from different hardware systems

Platform	Time required to get result (in seconds)
CPU, i3 processor, 8GB RAM	4.395
CPU, i5 processor, 8GB RAM	4.163
CPU, I7 processor, 8GB RAM	3.124
GPU, Nvidia K80	0.962

Time complexity of the proposed system architecture is tested on different hardware platforms [35]. The time required to get the result is tabulated in table 4.4.

5. Conclusion. From all the results, one can easily conclude that the proposed architecture is much accurate to detect the effect of chemotherapy treatment on the patient. It gives the necessity of chemotherapy or not. If the patient does not respond to the chemotherapy, then the proposed system itself provides suggestion to go for surgery. Moreover, system also correctly predicts the criticality level so proper medication can be suggested by the doctors. In this article, we examined the WDBC dataset utilizing dimensionality decrease strategies and three normal ML calculations to order dangerous and harmless cancers. Trial work has shown that arrangement execution relies upon the ML order strategy picked. Reproduction results show that SVMLDA and NNLDA are better than other ML classifier models. By the by, SVMLDA is picked over NNLDA on the grounds that NNLDA requires longer calculation time. Hence, this paper proposes a keen methodology that coordinates straight discriminant investigation and backing vector machines (utilizing the RBF piece) for bosom malignant growth finding. This chose approach has shown great and promising outcomes for approval datasets. Accomplished arrangement exactness of 98.82%, responsiveness of 98.41%, explicitness of 99.07%, and region under the recipient movement bend of 0.9994. This study shows that highlight determination and component extraction can assist with working on the finding of harmless and dangerous cancers utilizing AI procedures. Hence, this work presumes that coordinating critical dimensionality decrease strategies with ML grouping methods gives a superior way to deal with clinical determination (bosom malignant growth conclusion utilized as a contextual analysis). The primary thought is to consolidate dimensionality decrease with the advantages of the ML calculation. Future work might plan to form the picked approach into a potential viable

method for helping doctors in diagnosing bosom disease and aid a fast second assessment. Future work may likewise consider contrasting other ML calculations utilized with analyze bosom disease. Other illness choices may likewise be considered in ongoing examinations.

REFERENCES

[1] J. R. Benson and I. Jatoi., *The global breast cancer burden*, Future oncology, 2012, vol. 8, no. 6, pp. 697–702.

[2] L. J. Fallowfield, S. K. Leaity, A. Howell, S. Benson, and D. Cella., *Assessment of quality of life in women undergoing hormonal therapy for breast cancer: validation of an endocrine symptom subscale for the fact-b*, Breast cancer research and treatment, 1999, vol. 55, no. 2, pp. 187– 197.

[3] A. R. Costa, F. Fontes, S. Pereira, M. Gonc¸alves, A. Azevedo, and N. Lunet., *Impact of breast cancer treatments on sleep disturbances– a systematic review*, The Breast, 2014, vol. 23, no. 6, pp. 697–709.

[4] J. E. Carroll, K. Van Dyk, J. E. Bower, Z. Scuric, L. Petersen, R. Schiestl, M. R. Irwin, and P. A. Ganz., *Cognitive performance in survivors of breast cancer and markers of biological aging*, Cancer, 2019, vol. 125, no. 2, pp. 298–306.

[5] P. Minicozzi, L. Van Eycken, F. Molinie, K. Innos, M. Guevara, R. Marcos-Gragera, C. Castro, E. Rapiti, A. Katalinic, A. Torrella et al., *Comorbidities, age and period of diagnosis influence treatment and outcomes in early breast cancer*, International journal of cancer, 2019, vol. 144, no. 9, pp. 2118–2127.

[6] J. Teng, A. Abdygametova, J. Du, B. Ma, R. Zhou, Y. Shyr, and F. Ye., *Bayesian inference of lymph node ratio estimation and survival prognosis for breast cancer patients*, IEEE Journal of Biomedical and Health Informatics, 2019, pp. 1–1.

[7] P. V. C. Souza, A. G. dos Reis, G. R. R. Marques, A. J. Guimaraes, V. J. S. Araujo, V. S. Araujo, T. S. Rezende, L. O. Batista, and G. A. da Silva., *Using hybrid systems in the construction of expert systemsin the identification of cognitive and motor problems in children and young people*, in 2019 IEEE International Conference on Fuzzy Systems (FUZZ-IEEE), June 2019, pp. 1–6.

[8] C.-W. Han., *Fuzzy neural network-based fetal health monitoring using cardiotocography data*, in AIP Conference Proceedings, vol. 2104, no. 1. AIP Publishing, 2019, p. 030008.

[9] Y. Liu, S. Wu, Kuang-Pen Chou, Y. Lin, Jie Lu, Guangquan Zhang, Wen-Chieh Lin, and C. Lin., *Driving fatigue prediction with pre-event electroencephalography (eeg) via a recurrent fuzzy neural network*, in 2016 IEEE International Conference on Fuzzy Systems (FUZZ-IEEE), July 2016, pp. 2488–2494.

[10] P. V. d. C. Souza and A. J. Guimaraes., *Using fuzzy neural networks for improving the prediction of children with autism through mobile devices*, in 2018 IEEE Symposium on Computers and Communications (ISCC), June 2018, pp. 01 086–01 089.

[11] A. J. Guimaraes, V. J. S. Araujo, V. S. Araujo, L. O. Batista, and P. V. ˜ de Campos Souza., *A hybrid model based on fuzzy rules to act on the diagnosed of autism in adults*, in Artificial Intelligence Applications and Innovations, J. MacIntyre, I. Maglogiannis, L. Iliadis, and E. Pimenidis, Eds. Cham: Springer International Publishing, 2019, pp. 401–412.

[12] P. V. de Campos Souza, A. J. Guimaraes, V. S. Araujo, T. S. Rezende, and V. J. S. Araujo., *Using Fuzzy Neural Networks Regularized to Support Software for Predicting Autism in Adolescents on Mobile Devices*, Singapore: Springer Singapore, 2019, pp. 115–133.

[13] V. J. Silva Araujo, A. J. Guimar aes, P. V. de Campos Souza, ˜ T. Silva Rezende, and V. Souza Araujo., *Using resistin, glucose, age ´ and bmi and pruning fuzzy neural network for the construction of expert systems in the prediction of breast cancer*, Machine Learning and Knowledge Extraction, 2019, vol. 1, no. 1, pp. 466–482.

[14] Uddaraju, Susmitha, and M. Narasingarao., *A survey of machine learning techniques applied for breast cancer prediction*, International Journal of Pure and Applied Mathematics, 2017, 117.19, pp. 499-507.

[15] Susmitha, Uddaraju., *a review of machine learning frameworks for early and accurate prediction of neoadjuvant chemotherapy responses*, European Journal of Molecular & Clinical Medicine, 2020, 7.4, pp. 1040-1050.

[16] Uddaraju, Susmitha, and M. R. Narasingarao., *Predicting the Ductal Carcinoma Using Machine Learning Techniques—A Comparison*, Journal of Computational and Theoretical Nanoscience, 2019, 16.5-6, pp. 1902-1907.

[17] S. L. Bangare, S. T. Patil et al., *Implementing Tumor Detection and Area Calculation in MRI Image of Human Brain Using Image Processing Techniques*, Int. Journal of Engineering Research and Applications ISSN: 2248-9622, Vol. 5, Issue 4, (Part -6) April 2015, pp.60-65.

[18] K. Gulati et. al., *Use for Graphical User Tools in Data Analytics and Machine Learning Application*, Turkish Journal of Physiotherapy and Rehabilitation; 32(3), ISSN 2651-4451, e-ISSN 2651-446X.

[19] LMI Leo Joseph et. Al., *Methods to Identify Facial Detection in Deep Learning Through the Use of Real-Time Training Datasets Management*, EFFLATOUNIA - Multidisciplinary Journal, ISSN:1110-8703, Volume 5, Issue 2, pp.1298 -1311.

[20] G. Awate et. al., *Detection of Alzheimers Disease from MRI using Convolutional Neural Network with Tensorflow*, https://arxiv.org/abs/1806.10170.

[21] Shachi Mall et. al., em Implementation of machine learning techniques for disease diagnosis, Materials Today: Proceedings, 2021, ISSN 2214-7853, https://doi.org/10.1016/j.matpr.2021.11.274.

[22] *Breast cancer in young women by Australian government*, Breast cancer in young women statistics | Breast Cancer in Young Women (canceraustralia.gov.au).

Edited by: Vinoth Kumar
Received: Jun 21, 2022
Accepted: Dec 2, 2022